8-15-1972

Hydrostatic Oxygen Burning in Stars. II. Oxygen Burning at Balanced Pwer

S E. Woosley
Rice University

W David Arnett
Rice University

Donald D. Clayton
Clemson University, claydonald@gmail.com

THE ASTROPHYSICAL JOURNAL, 175:731–749, 1972 August 15

HYDROSTATIC OXYGEN BURNING IN STARS. II. OXYGEN BURNING AT BALANCED POWER

S. E. WOOSLEY, W. DAVID ARNETT,* AND DONALD D. CLAYTON
Institute of Theoretical Astronomy, Cambridge, England, and Rice University, Houston, Texas
Received 1972 February 1

ABSTRACT

The nucleosynthesis that occurs during hydrostatic oxygen burning in a "typical" stellar zone is examined in detail under the assumption that such stellar zones are in an approximate state of *balanced power* from $^{16}O + {}^{16}O$ energy generation and from neutrino (or photon) energy loss. Special attention is paid to the amount of neutron enrichment that occurs and the implications for nucleosynthesis theory. Accuracy of a common approximation for $^{16}O + {}^{16}O$ energy generation is discussed also.

Theoretical models which assume the existence of a direct e-ν coupling in the weak interaction give results that are more consistent with current ideas regarding stellar nucleosynthesis than models which do not.

I. INTRODUCTION

The behavior of an oxygen star of mass M resembles that of a more realistic stellar model which has an oxygen core of the same mass ($M_{\rm core} = M$). In the first paper of this series (Arnett 1972, henceforth referred to as Paper I), the hydrostatic evolution of oxygen stars of various masses ($M/M_\odot = 2$, 4, 8, and 16) was considered in detail. One of the most important results of the investigation was the observation that the temperature and density in a "typical" zone could be specified during most of the oxygen-burning stage by a balanced power constraint of the form

$$\epsilon(T_9, \rho, X_i) \approx s(T_9, \rho, X_i), \tag{1}$$

where ϵ is the rate of nuclear energy generation and s is the rate of energy loss due to neutrinos and both rates are functions of T_9 (the temperature in billions of degrees), ρ (density in g cm^{-3}), and composition X_i. The meaning of the word "typical" is discussed in Paper I; it was found that equation (1) should be good to within about a factor of 3 for a zone which has a nuclear evolution representative of the convective core during oxygen burning. Once oxygen is ignited, the zone also satisfies the relation (Paper I, eq. [11])

$$\rho \propto T_9^3 . \tag{2}$$

By combining equations (1) and (2) the history of the zone is uniquely specified by a choice of initial conditions. It will be the purpose of this paper to investigate in detail the nucleosynthesis that occurs in such zones for a variety of initial conditions that should approximate the actual situation in stellar cores of various mass. We shall examine the changes in composition that occur as a result of both strong and weak nuclear interactions as the star evolves. In particular, we shall be concerned with the evolution of η, the neutron-excess parameter, defined by

$$\eta \equiv \Sigma(N_i - Z_i) Y_i \tag{3}$$

where N_i and Z_i are the neutron and proton numbers, respectively, of the species i and Y_i is the species' mass fraction divided by its atomic weight (mass fraction per nucleon).

* Alfred P. Sloan Foundation Fellow. Present address: Department of Astronomy, University of Texas, Austin, Texas 78712.

Many calculations of the nucleosynthesis that might be expected to occur in an exploding star (see, for example, Arnett and Clayton 1970; Arnett 1969*a*, 1971; Truran and Arnett 1970, 1971; Woosley, Arnett, and Clayton 1972) have shown that the resultant abundances to come out of such an explosion agree well with the observed natural abundances of the elements only if the parameter η takes on values in a very restricted range near 0.002. We shall thus be interested in determining what sets of initial conditions (i.e., what masses of stars) can yield values of η commensurate with this requirement. Since this determination will rest upon the choice of a particular set of reaction cross-sections, we tabulate those rates which we feel to be important in table 1. Most of these do not have direct experimental determinations; therefore, examination of these rates by those interested in accurate laboratory measurement would be quite useful. As a by-product of this investigation we will determine the accuracy of the simple approximation to the rate of nuclear energy generation used in Paper I. Only in the region where the energy-generation rate, determined by the evolution of the nuclear reaction network, agrees well with the simple approximation is the decoupling of the hydrostatic evolution from the detailed thermonuclear evolution a good approximation.

II. NUMERICAL TECHNIQUE

The technique employed here for following the composition evolution is the same as that employed by Arnett and Truran (1969) for hydrostatic carbon burning. A "reaction network" of coupled differential equations is set up that specifies the time behavior of all species which may accumulate in any sizable abundance during the nuclear evolution. The terms in the differential equations represent "flows" from one species to another by various nuclear reactions. This set of equations is linearized and evolved forward in time by matrix inversion. The reaction network employed for these calculations is shown in figure 1. Each species shown is coupled to its neighbors by all possible strong binary interactions involving a single neutron, proton, α-particle, or photon in an entrance or exit channel. In addition, all possible links due to the weak interactions (electron capture, positron emission, and β-decay) are included. Also included are the triple-α, $^{12}C + {}^{12}C$, $^{16}O + {}^{16}O$, and $^{12}C + {}^{16}O$ reactions. The values employed for the weak-interaction rates were taken from Hansen (1968). Strong-interaction rates come from a wide variety of sources and reflect the current state of the data analysis. Representative values and sources are included in table 1. The choice of elements to be included in the network was determined by the conditions that are expected to prevail during hydrostatic oxygen burning. For temperatures less than $T_9 = 2.5$, only very small abundances of elements having $Z > 20$ accumulate; therefore, the network terminates at titanium. The coupling among species in the mass range $24 \leq A \leq 44$ is the most extensive because this is the range of masses which should accumulate to sizable abundance during the burning. Large numbers of neutron-rich species are included so that the evolution may be followed accurately in regions of increasing neutron excess η. This particular network should be reasonably correct for values of η up to about 0.05. Below $A = 24$, the only reaction that really matters is $^{16}O + {}^{16}O$; therefore, the network is quite sparse in that region.

This network of equations is evolved forward in time along the path specified by equations (1) and (2) by inversion of the linearized matrix at successive time steps. The size of the individual time step is determined by the criterion that no species of mass fraction larger than 10^{-7} is allowed to vary more than 15 percent during one time step. This criterion was tested and found to result in cumulative errors of no more than 5 percent in the mass fractions of abundant species during the course of nuclear evolution.

Calculations were carried out for two different initial compositions. One was pure oxygen which we shall denote in this discussion as composition A. The other was taken to represent what might be the typical ashes of hydrostatic carbon burning in the zone. Under the assumption that helium burning leads to roughly equal amounts of ^{12}C and

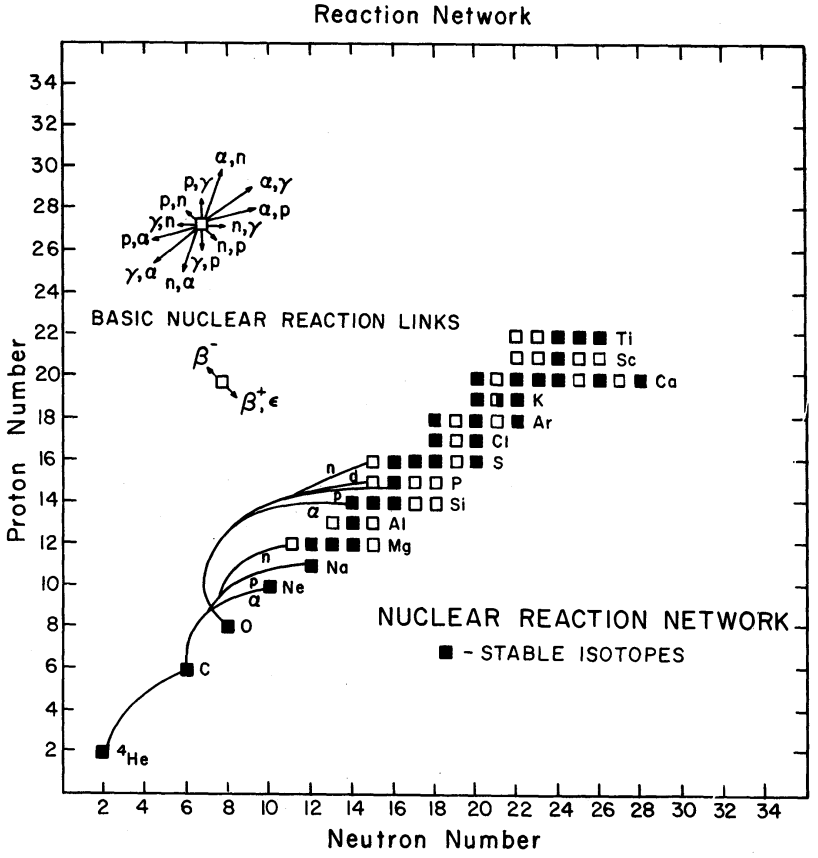

FIG. 1.—Nuclear reaction network for hydrostatic oxygen burning. *Solid squares*, terrestrially stable nuclei; *open squares*, unstable nuclei. These nuclei are coupled by all possible reactions of the type illustrated.

^{16}O by weight, Arnett and Truran (1969) have calculated the nucleosynthesis which would occur during hydrostatic carbon burning for a range of temperatures and at a density which they considered appropriate ($T_9 = 0.6$–1.4, $\rho = 5 \times 10^5$). Assuming that the increase in temperature following carbon burning results in the rearrangement of all ^{20}Ne produced into roughly equal amounts of ^{16}O and ^{24}Mg, Truran and Arnett (1970) suggest that a composition typical of a zone which has undergone hydrostatic carbon burning in a Population I star might be: $X(^{16}O) = 0.54$, $X(^{24}Mg) = 0.32$–13η, $X(^{26}Mg) = 13\eta$, and $X(^{28}Si) = 0.14$. This composition, with $\eta = 1.54 \times 10^{-3}$, will be referred to as composition B. Calculations were also carried out employing initial compositions having $\eta = 0$ and $\eta = 3.08 \times 10^{-3}$. These are referred to as compositions C and D, respectively.

In actual practice a simplified version of the balanced power constraint given in equation (1) was employed for iteration to obtain the path of the evolution in the (ρ, T_9)-plane. A less general form of the energy-generation rate was used which depends only on the ^{16}O abundance, not on the entire composition. The prescription was the same as that employed in Paper I. This simplification has the additional appeal of allowing comparison of the approximation employed for this rate with the actual energy-generation rate which may be obtained at each time step by examination of the time derivatives of *all* the species in the network. Thus a measure of the accuracy of the simple representation of ϵ may be obtained. The composition dependence of the neutrino rate was also greatly simplified. Under the conditions of hydrostatic oxygen burn-

TABLE 1

IMPORTANT REACTION RATES*

Target	Reaction	$N_A \langle \sigma v \rangle$ Forward Rate T_9=1.8	Forward Rate T_9=2.0	Reverse Rate T_9=1.8	Reverse Rate T_9=2.0	Ref.
α	3α	5.2(-11)	4.9(-11)	1.6(- 9)	2.2(- 7)	1,2
^{12}C	$^{12}C + ^{12}C$	2.3(- 5)	2.1(- 4)	...	...	2,3
	$^{12}C + ^{16}O$	1.8(- 8)	2.6(- 7)	...	...	2,4
	(α,γ)	3.2(- 4)	9.7(- 4)	3.5(-13)	1.3(-10)	1
^{16}O	$^{16}O + ^{16}O$†	3.8(-13)	1.3(-11)	...	...	2,5
	(α,γ)	2.4(- 1)	3.9(- 1)	1.8(- 3)	7.5(- 2)	1
^{20}Ne	(α,p)	5.0(- 2)	3.3(- 1)	1.8(+ 5)	2.6(+ 5)	1
	(α,γ)	1.8(0)	3.9(0)	2.1(-15)	2.2(-12)	1
^{23}Na	(p,γ)	6.8(+ 3)	8.3(+ 3)	2.2(-18)	6.0(-15)	1
	(α,p)	5.3(0)	1.5(+ 1)	5.5(- 4)	4.9(- 3)	1
^{23}Mg	$(e^+\nu)$	5.1(- 2)	4.9(- 2)	...	...	6
^{24}Mg	(n,γ)	8.3(+ 4)	9.2(+ 4)	1.8(- 6)	2.7(- 4)	7
	(α,p)	9.6(- 1)	4.2(0)	1.6(+ 4)	2.5(+ 4)	1
	(α,γ)	4.2(- 1)	9.5(- 1)	7.0(-18)	1.2(-14)	1
^{25}Mg	(n,γ)	1.9(+ 5)	1.9(+ 5)	4.2(-15)	6.5(-12)	7
	(p,γ)	4.9(+ 3)	6.1(+ 3)	2.8(- 3)	2.4(- 1)	1
	(α,p)	9.4(- 2)	4.9(- 1)	4.4(+ 3)	1.1(+ 4)	7
	(α,n)	2.0(0)	7.3(0)	1.5(- 6)	3.0(- 5)	7
^{26}Mg	(p,γ)	6.9(+ 3)	8.5(+ 3)	3.6(-10)	1.1(- 7)	1
	(α,n)	2.4(0)	8.8(0)	3.3(0)	1.2(+ 1)	7
^{26}Al	$(e^+\nu)$	2.8(- 3)	2.9(- 3)	...	...	6
^{27}Al	(n,γ)†	1.6(+ 5)	1.8(+ 5)	9.6(- 6)	1.8(- 3)	7
	(p,γ)†	2.4(+ 3)	3.4(+ 3)	2.5(-18)	7.1(-15)	1
	(α,p)	1.1(0)	3.5(0)	4.8(- 6)	7.2(- 5)	1
	(α,n)	9.8(- 3)	7.0(- 2)	1.7(6)	2.2(+ 6)	7
	(α,γ)	8.9(- 3)	3.2(- 2)	3.5(-18)	7.5(-15)	7
^{28}Al	(p,n)†	1.0(+ 6)	1.7(+ 6)	1.6(- 5)	3.3(- 4)	7
	$(e^-\bar{\nu})$†	3.0(- 3)	3.0(- 3)	...	...	6
^{28}Si	(n,γ)	1.1(+ 5)	1.2(+ 5)	4.4(- 9)	1.4(- 6)	7
	(α,p)	5.2(- 2)	2.9(- 1)	2.1(+ 4)	3.3(+ 4)	1
	(α,γ)	3.1(- 2)	8.2(- 2)	1.7(-10)	4.7(- 8)	1
^{29}Si	(n,γ)	1.6(+ 5)	1.8(+ 5)	2.8(-14)	3.4(-11)	7
	(p,γ)†	1.6(+ 3)	2.0(+ 3)	1.1(- 2)	5.6(- 1)	1
	(α,p)	9.3(- 5)	9.9(- 4)	1.6(+ 3)	3.5(+ 3)	7
	(α,n)	1.5(- 1)	7.0(- 1)	2.0(+ 4)	3.4(+ 4)	7
	(α,γ)	4.5(- 3)	1.5(- 2)	4.2(-12)	1.6(- 9)	7
^{30}Si	(n,γ)	4.2(+ 4)	4.7(+ 4)	1.6(- 4)	1.5(- 2)	7
	(p,n)	4.1(- 6)	1.1(- 4)	1.6(+ 8)	1.8(+ 8)	7
	(p,γ)	3.2(+ 3)	4.3(+ 3)	2.9(- 7)	5.0(- 5)	1
	(α,p)	1.6(- 5)	2.0(- 4)	5.8(+ 3)	1.0(+ 4)	7
	(α,n)†	1.3(- 3)	1.3(- 2)	7.1(+ 6)	7.9(+ 6)	7
	(α,γ)	2.6(- 2)	9.1(- 2)	2.8(-13)	1.9(-10)	1

TABLE 1—*Continued*

Target	Reaction	$N_A \langle \sigma v \rangle$				Ref.
		Forward Rate		Reverse Rate		
		T_9=1.8	T_9=2.0	T_9=1.8	T_9=2.0	
^{31}Si	$(e^-\bar{\nu})$	6.5(- 5)	6.5(- 5)	...	...	6
^{30}P	(p,γ)†	1.4(+ 3)	1.9(+ 3)	8.7(- 4)	7.0(- 2)	7
	$(e^+\nu)$†	4.0(- 3)	4.4(- 3)	...	...	6
^{31}P	(n,γ)	1.6(+ 5)	1.8(+ 5)	2.8(- 7)	6.2(- 5)	7
	(p,γ)	7.9(+ 2)	1.1(+ 3)	1.1(-11)	5.3(- 9)	1
	(α,p)	5.6(- 2)	2.2(- 1)	6.6(- 3)	3.9(- 2)	1
^{32}P	(p,n)	5.7(+ 4)	1.1(+ 5)	4.3(+ 2)	1.4(+ 3)	7
	$(e^-\bar{\nu})$	6.5(- 6)	6.5(- 6)	...	...	6
^{31}S	$(e^+\nu)$†	2.5(- 1)	2.5(- 1)	...	...	6
^{32}S	(n,γ)	4.6(+ 5)	4.8(+ 5)	3.3(- 9)	1.1(- 6)	7
	(α,p)	3.9(- 2)	2.3(- 1)	5.5(+ 3)	9.6(+ 3)	1
	(α,γ)	5.4(- 4)	2.1(- 3)	2.2(-11)	7.0(- 9)	1
^{33}S	(n,γ)†	3.6(+ 5)	3.8(+ 5)	6.7(-16)	1.3(-12)	7
	(α,p)	5.3(- 4)	4.2(- 3)	3.7(+ 2)	8.5(+ 2)	7
	(α,n)	5.9(- 3)	3.4(- 2)	3.3(+ 4)	5.2(+ 4)	7
	(α,γ)	1.8(- 3)	6.6(- 3)	2.7(-11)	9.3(- 9)	7
	(e^-,ν)†	3.2(- 7)	4.2(- 7)	...	...	6
^{34}S	(n,γ)	9.4(+ 4)	1.1(+ 5)	2.9(- 5)	3.4(- 3)	7
	(p,γ)	4.2(+ 2)	6.3(+ 2)	7.0(- 6)	7.6(- 4)	1
	(α,p)	4.1(- 5)	4.9(- 4)	1.1(+ 4)	1.9(+ 4)	1
	(α,n)	2.1(- 6)	4.6(- 5)	1.7(+ 7)	1.9(+ 7)	7
	(α,γ)	1.3(- 2)	5.0(- 2)	1.4(-11)	6.4(- 9)	1
^{35}S	(p,n)	3.2(+ 4)	6.3(+ 4)	1.7(+ 6)	2.2(+ 6)	7
^{36}S	(p,n)	3.1(+ 2)	1.2(+ 3)	1.5(+ 7)	1.6(+ 7)	7
	(p,γ)	6.4(+ 3)	9.7(+ 3)	2.2(-10)	8.7(- 8)	7
^{35}Cl	(n,γ)	7.1(+ 5)	7.2(+ 5)	2.4(- 8)	7.3(- 6)	7
	(p,γ)	8.0(+ 2)	1.1(+ 3)	2.3(-10)	9.0(- 8)	1
	(e^-,ν)	8.8(- 7)	1.1(- 6)	...	...	6
^{36}Cl	(p,n)	2.0(+ 4)	3.7(+ 4)	1.5(+ 5)	2.8(+ 5)	7
^{37}Cl	(p,n)	1.1(+ 3)	3.6(+ 3)	3.3(+ 7)	3.8(+ 7)	7
	(p,γ)	2.4(+ 3)	3.7(+ 3)	9.1(-15)	1.3(-11)	1
^{36}Ar	(n,γ)	2.2(+ 5)	2.4(+ 5)	6.1(-10)	2.3(- 7)	7
	(α,p)	9.0(- 4)	5.8(- 3)	3.4(0)	9.3(0)	7
^{37}Ar	(n,γ)	1.8(+ 5)	2.0(+ 5)	2.2(-17)	5.9(-14)	7
	(e^-,ν)	8.4(- 6)	9.5(- 6)	...	...	6
^{38}Ar	(n,γ)	8.0(+ 4)	9.0(+ 4)	1.6(- 4)	1.5(- 2)	7
	(p,γ)	9.4(+ 2)	1.5(+ 3)	1.5(- 5)	1.7(- 3)	7
	(α,γ)	1.4(- 3)	7.0(- 3)	7.1(-10)	2.4(- 7)	7

NOTES TO TABLE 1

* All nuclear reactions shown in figure 1 but not listed here were deemed to be of only secondary interest to hydrostatic oxygen burning. The rates for all these unlisted reactions were taken from sources (7) for strong interactions and (6) for weak interactions.

† Reaction rate very important to the determination of the change in neutron excess that occurs during hydrostatic oxygen burning. See text.

1. Fowler, Caughlan, and Zimmerman (1971).
2. The rate given is the rate of formation of the compound nucleus.
3. Patterson, Winkler, and Zaidins (1970). Branching ratios assumed are $B_\alpha = 0.66$, $B_p = 0.32$, $B_n = 0.02$.
4. Patterson *et al.* (1971) and Woosley, Arnett, and Clayton (1971). Branching ratios assumed are $B_\alpha = 0.40$, $B_p = 0.50$, $B_n = 0.10$.
5. Spinka and Winkler (1972). Branching ratios assumed are $B_\alpha = 0.34$, $B_p = 0.56$, $B_n = 0.05$, $B_d = 0.05$.
6. Hansen (1968). The number shown is the inverse lifetime of the target against the reaction listed at a density $\rho = 10^6$ g cm^{-3}.
7. Calculation based on nuclear systematics by Truran (1971).

ing the processes contributing to neutrino losses may be pair production, plasma-neutrino production, photoneutrino production, and neutrino emission from weak interactions involving the nuclei that are present. The first three depend only upon the temperature, density, and atomic weight per electron μ_e, defined by $(\mu_e)^{-1} = \Sigma Z_i Y_i = (1 - \eta)/2$. If approximate equality of neutrons and protons prevails, then $\mu_e \approx 2$. The emission of neutrinos from nuclear weak interactions depends more critically upon the composition. If such losses were negligible the composition dependence of s would be extremely simple. Neutrino-loss rates due to electron capture, β-decay, and positron emission for elements which might be present during the nuclear evolution were calculated using the rates of Hansen (1968) for a range of temperatures and densities that are pertinent to oxygen burning. In all cases considered here the losses were less than 1 percent of the combined plasma, pair, and photoneutrino loss rate given by Beaudet, Petrosian, and Salpeter (1967). Thus composition dependence of s can be ignored. Then equation (1) takes on the somewhat simplified form,

$$\tilde{\epsilon}[\rho, T_9, X(^{16}\mathrm{O})] = s[\rho, T_9], \tag{4}$$

where $\tilde{\epsilon}$ is the simple approximation used in Paper I for the rate of nuclear energy generation and s is the neutrino loss rate given by Beaudet, Petrosian, and Salpeter with $\mu_e = 2$. Assuming initial values for two of the three variables ρ, T_9, and $X(^{16}\mathrm{O})$, fixes the third. The initial temperatures required by various choices of initial density and oxygen abundance are shown in table 2. The subsequent evolution is then uniquely specified. Knowing ρ, T_9, and the abundance of $^{16}\mathrm{O}$ by mass fraction, $X(^{16}\mathrm{O})$, at time t^n one steps forward in time to a new oxygen abundance by inverting the reaction network matrix. Equation (4) is then solved to obtain the new temperature and density at t^{n+1}, and the process continues.

The actual rate of nuclear energy generation at each time step is calculated by examining the changes in abundance of all species in the network. Thus it is a simple matter to examine the accuracy to which $\tilde{\epsilon}$ represents the actual energy-generation rate. The actual energy-generation rate and the fractional variance of $\tilde{\epsilon}$—that is $(\epsilon - \tilde{\epsilon})/\epsilon$—are shown in figure 2 for typical runs employing two different initial compositions. Until $^{16}\mathrm{O}$ is mostly depleted, the agreement between ϵ and $\tilde{\epsilon}$ is good, the error amounting to no more than 20 percent for either initial composition. The actual energy-generation rate is somewhat underestimated for composition B by $\tilde{\epsilon}$. This is due to the fact that the chief product of composition B is $^{28}\mathrm{Si}$ rather than $^{32}\mathrm{S}$. Thus somewhat less energy is liberated. The steep rise in ϵ at $^{16}\mathrm{O}$ depletion is due to the rapidly rising temperature.

The temperature history of two runs is shown in figure 3. There is a dramatic rise in temperature as the oxygen is consumed. For very small oxygen mass fractions this curve is inaccurate. As the oxygen disappears, oxygen burning ceases to be the dominant reaction and $\tilde{\epsilon}$ is no longer a valid approximation to the actual rate of energy generation. For small values of $X(^{16}\mathrm{O})$ the rise in temperature should not be quite so large as indicated in figure 3.

TABLE 2

TEMPERATURES AND DENSITIES FOR $s = \tilde{\epsilon}$

$X(^{16}\mathrm{O})$	T_9	$\rho/10^6$	$X(^{16}\mathrm{O})$	T_9	$\rho/10^6$
1.0.....	2.00	1	0.54.....	2.11	1
1.0.....	1.88	2	0.54.....	1.98	2
1.0.....	1.80	3	0.54.....	1.90	3
1.0.....	1.74	4	0.54.....	1.84	4
1.0.....	1.70	5	0.54.....	1.80	5

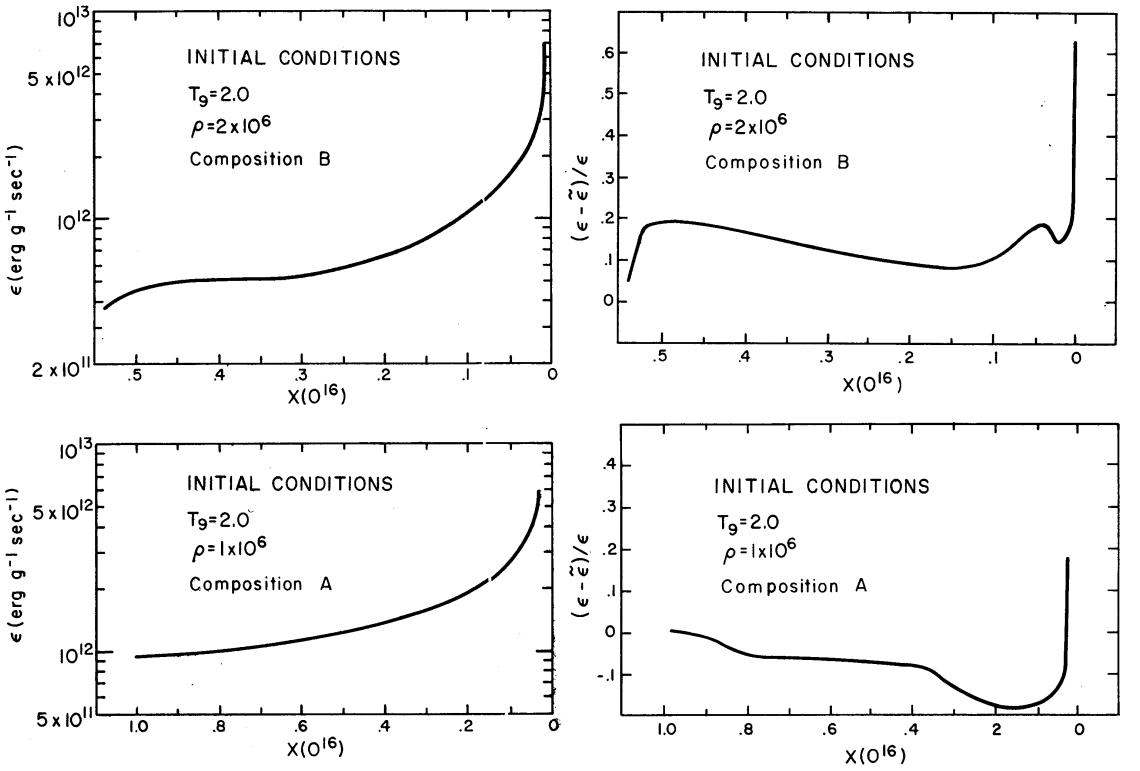

FIG. 2.—Nuclear energy generation during hydrostatic oxygen burning. The actual rate of energy generation and the fractional error in the representation of the energy generation rate by $\tilde{\epsilon}$ are shown as functions of the ^{16}O mass fraction for "balanced power" runs employing the conditions shown.

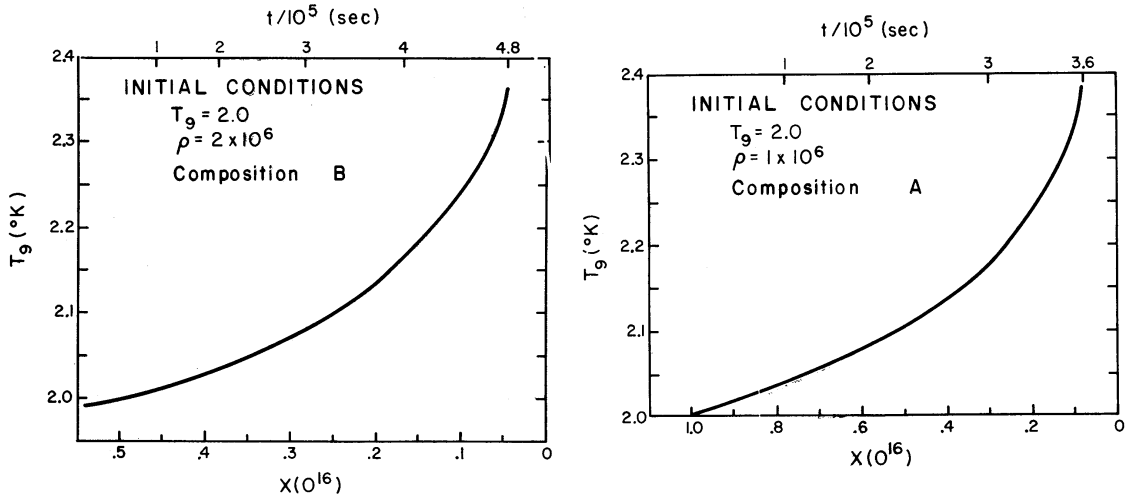

FIG. 3.—Thermal history during hydrostatic oxygen burning. The temperature obtained from the balanced-power assumption is shown as a function of time and ^{16}O mass fraction for the initial conditions shown.

III. NUCLEOSYNTHESIS

Nucleosynthesis calculations were carried out for compositions A and B and a variety of initial temperatures in the range $1.8 \leq T_9 \leq 2.1$. This range was thought to span adequately the range of temperatures encountered for the models in Paper I when ^{16}O had not been significantly depleted. Thus these calculations should be pertinent to oxygen stars in the mass range 2–16 $M_\odot$.

Dominant nuclear flows for oxygen burning with an initial temperature $T_9 = 2.0$ are shown for compositions A and B in figures 4*a* and 4*b* (at an oxygen depletion of about 10 percent). The nuclear evolution at this point is obviously composition dependent. In the case of initial composition A the dominant net flow is

$$^{16}O + {}^{16}O \rightarrow {}^{28}Si + \alpha \rightarrow {}^{32}S \qquad \text{(composition A)}.$$

Although a few free α-particles are going onto ^{16}O with the net production of some ^{28}Si via $^{16}O(\alpha, \gamma)^{20}Ne(\alpha, \gamma)^{24}Mg(\alpha, \gamma)^{28}Si$, the chief product at this point is ^{32}S. It is significant to note that although composition A started with no neutron enrichment, a surplus of neutrons is being created by $^{31}S(e^+\nu)^{31}P$ with the result that neutron-rich isotopes such as ^{29}Si, ^{30}Si, and ^{33}S are being produced. Flows for composition B are substantially different. The principal net flows here are

$$^{16}O + {}^{16}O \rightarrow {}^{28}Si + \alpha\,, \qquad {}^{24}Mg + \alpha \rightarrow {}^{28}Si + \gamma \qquad \text{(composition B)}.$$

The cross-section for alpha capture by ^{24}Mg under oxygen-burning conditions is much greater than that by ^{28}Si. As a result, almost all alphas produced will be added onto ^{24}Mg until its initial abundance is depleted. At this point ^{28}Si is almost the exclusive product of the burning. The chief source of neutrons here is the initial abundance of ^{26}Mg even though $^{31}S(e^+\nu)^{31}P$ is still quite active. As the magnesium isotopes become exhausted, the qualitative behavior of the evolution of composition B becomes more like that of composition A, resulting in the buildup of species heavier than silicon. The final results will be less alpha-rich for composition B (that is, lower abundances for ^{32}S, ^{36}Ar, ^{40}Ca, and their isotopes relative to ^{28}Si), due to the initial presence of the "alpha poison" ^{24}Mg.

Throughout the burning the strong nuclear flows are very similar to those that would be obtained from similar calculations for a nuclear evolution employing a constant temperature, differing only when the ^{16}O mass fraction has dropped significantly. Even in this case the flows are basically the same except that there is an overall decrease in the timescale as the temperature increases. As a result, weak interactions (which under these conditions are less temperature sensitive than the strong interactions) may be important earlier in the evolution but become negligible as the temperature increases. Hence η may increase for a time but eventually reaches a maximum value as the timescale for dominant strong interactions becomes much shorter than typical weak-interaction timescales.

The evolution of composition for the two runs which employed initial temperature $T_9 = 2.0$ is shown in figure 5. The chief product resulting from the burning of composition B is ^{28}Si while composition A is dominated by ^{32}S (at least at low temperatures). This is a composition effect only and was seen by Arnett (1969*b*). It was found to occur in all runs regardless of initial temperature and density (within the range considered) and has an interesting implication for stellar evolution. If the zone has previously undergone carbon burning—that is, if its composition is adequately reflected by composition B—then the overwhelming product of hydrostatic oxygen burning is ^{28}Si and oxygen burning merges smoothly into silicon burning in a normal fashion. But if the zone's initial composition is almost entirely pure oxygen, a great overabundance of ^{32}S is produced relative to ^{28}Si. As the oxygen begins to deplete, it becomes less efficient as an alpha-producing source and the alpha density drops. Photodisintegration of ^{32}S [via $^{32}S(\gamma, \alpha)^{28}Si$

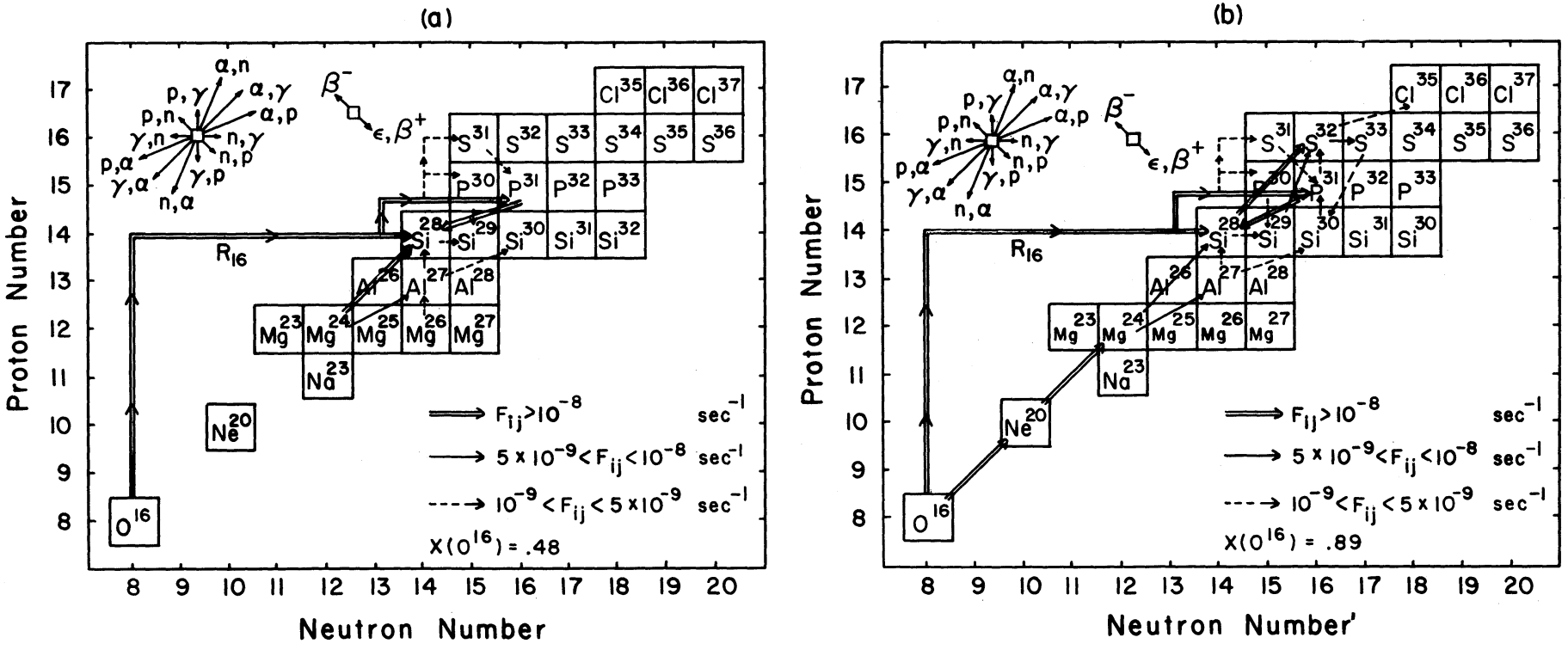

FIG. 4*a*.—Major flows in hydrostatic oxygen burning. This figure shows the major *net* (forward minus reverse) flows at a time 7.44×10^4 seconds into the burning of composition B, which employed an initial temperature $T_9 = 2$ and density $\rho = 2 \times 10^6$. The type of reaction represented by the vector is given by the key in the upper left corner of the figure. The principal species being produced at this point is ^{28}Si. The dominant weak interaction is the positron decay of ^{31}S.

FIG. 4*b*.—Major flows in hydrostatic oxygen burning. This figure shows the major net flows at a time 4.8×10^4 s into the burning of composition A, which employed an initial temperature $T_9 = 2$ and density $\rho = 1 \times 10^6$. The principal species being formed is ^{32}S. The dominant weak interaction is the positron decay of ^{31}S.

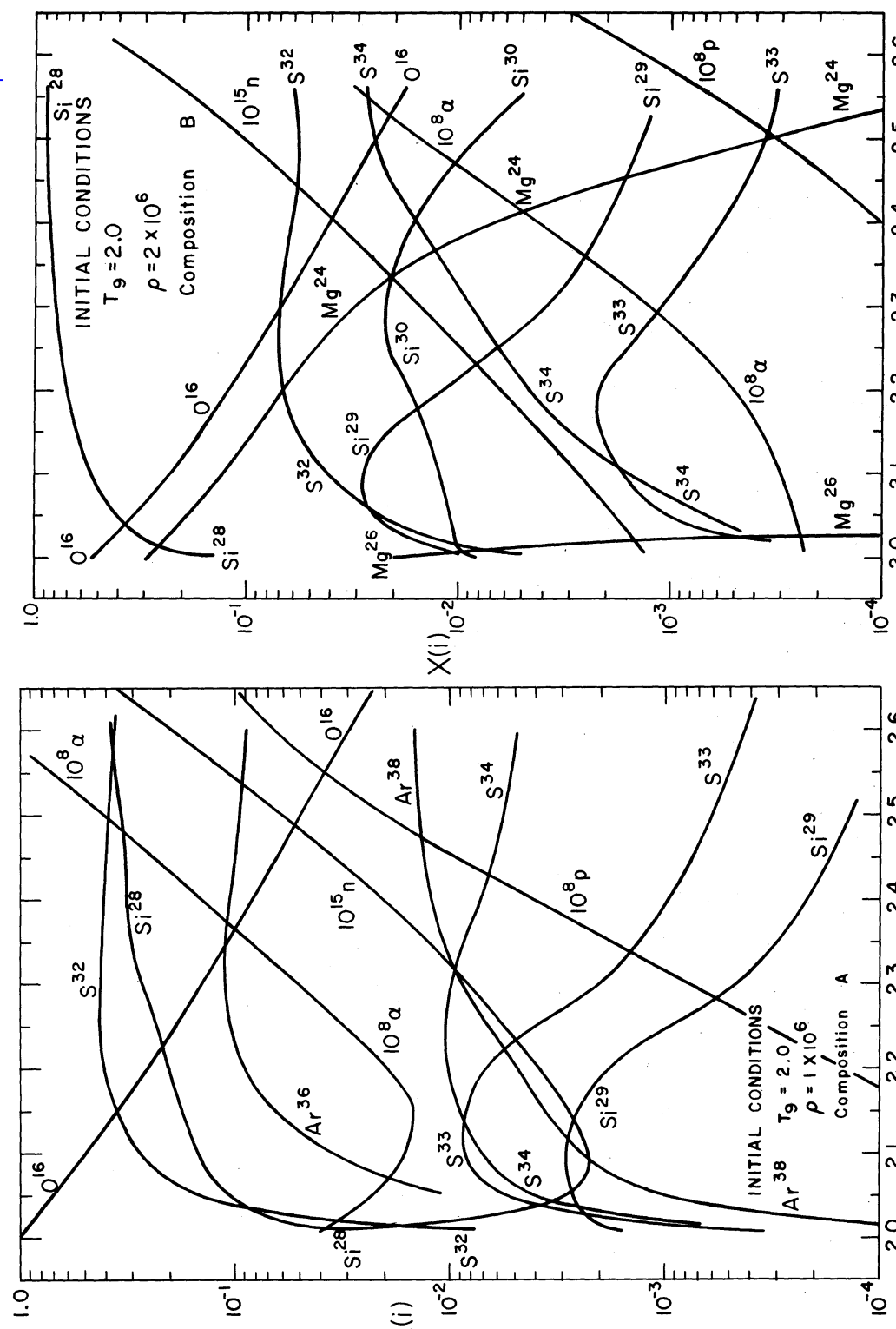

FIG. 5.—Composition history during hydrostatic oxygen burning. The abundances by mass fraction of important species are given as functions of the temperature. Also shown are the free-particle mass fractions which have been multiplied by various factors for display purposes. The initial conditions of the run are shown in the figures. Note similarity to fig. 10 of Arnett (1969*b*).

and $^{32}S(\gamma, p)^{31}P(p, \alpha)^{28}Si$] then exceeds the rates of the inverse reactions on ^{28}Si, and the abundance of ^{28}Si increases at the expense of ^{32}S. This process acts as a new source of alphas, most of which are captured onto ^{32}S. Thus the overall effect may be approximated by

$$2\,{}^{32}S \rightarrow {}^{32}S + {}^{28}Si + \alpha \rightarrow {}^{28}Si + {}^{36}Ar$$

(see also Fowler and Hoyle 1964). This process is slightly endoergic by 0.30 MeV and could rob the star of energy in the late stages of oxygen burning. The effect is somewhat analogous to the photodisintegration rearrangement which occurs for ^{20}Ne at the end of carbon burning, although in that case the net process is exoergic.

The final abundances at the end of oxygen burning are given in table 3. Oxygen burning was defined to be ended when the time derivative of either ^{28}Si or ^{32}S changed sign, that is, when the mass fraction of either began to decrease. *It should be emphasized that there can be no clear division between the end of oxygen burning and the onset of silicon burning*, but it is at this point that $\tilde{\epsilon}$ becomes a poor approximation to the actual rate of energy generation. Note that a significant amount of ^{16}O can remain when the "end of oxygen burning" is defined this way. The abundances given are merely representative of what must be a reasonable initial composition for the next stage of nuclear processing, They are not really suitable for comparison to solar-system abundances because this material is still tightly bound in the interior of a star and any ejection mechanism would most likely result in subsequent additional processing.

IV. NEUTRON ENRICHMENT

The value of η at the termination of oxygen burning is a very interesting quantity. Although the elemental composition may yet undergo a great deal of transformation, the overall neutron excess *should not decrease* during future burning stages. This is due to the fact that one is working with distributions of elements which lie for the most part to the proton-rich side of the valley of beta-stability. All subsequent weak interactions should tend to increase the neutron enrichment of the material. Therefore, we may regard the value of the neutron excess η, at the end of hydrostatic oxygen burning, as representing a lower bound (or more likely a near equality) to the value of η which characterizes the explosive nucleosynthesis to come out of such zones. The distribution of elements coming out of an exploding object will best approximate the measured solar abundances if $\eta \approx 0.002$. Any substantial increase in η, say beyond a factor of 2 of this value, results in severe distortion of the output distribution of explosive burning. Consider a star undergoing hydrostatic oxygen burning which is to explode and contribute substantially to the interstellar medium. In such an object, zones which have a substantial increase in η must not comprise any sizable fraction of the ejected mass. This means either that the star does not process oxygen under such conditions or that such zones must not be ejected but instead stay behind as part of a "remnant."

The changes in η which occur for various initial conditions are given in table 3. Assume that (1) a direct e-ν coupling exists and gives a loss rate near that represented by the analytic formulae of Beaudet *et al.* (1967), and (2) the nuclear cross-sections basic to this calculation are near the actual values. Then it is apparent that regardless of initial composition *the neutron mass excess in a zone that burns under conditions of approximate balanced power will be increased to an unacceptable degree if the initial temperature does not exceed* 1.8×10^9 ° *K*.

Figure 6 shows the weak flows that contribute to this change in η. The only significant reaction that acts to impede the increase in η is $^{28}Al(e^-\bar{\nu})^{28}Si$. Since the ^{28}Al is created by

$$^{24}Mg(\alpha, p)^{27}Al(n, \gamma)^{28}Al\,,$$

1972ApJ...175..731W

TABLE 3

FINAL ABUNDANCES BY MASS FRACTION AT THE END OF HYDROSTATIC OXYGEN BURNING

Composition	A				B				C	D
T_{9i}	1.8	1.9	2.0	2.1	1.8	1.9	2.0	2.1	1.9	1.9
$\rho_i/10^6$	3	2	1	.6	5	3	2	1	3	3
Initial η ($\times 10^3$)	0	0	0	0	1.54	1.54	1.54	1.54	0	3.08
$\Delta\eta(\times 10^3)$	6.72	3.27	1.20	.46	3.13	1.34	.73	.14	1.59	1.32
O^{16}	8.49(-2)	1.31(-1)	1.94(-1)	1.55(-1)	1.96(-3)	9.79(-3)	1.79(-2)	4.07(-2)	1.15(-2)	8.99(-3)
Si^{28}	2.95(-1)	2.59(-1)	2.32(-1)	2.74(-1)	8.84(-1)	8.86(-1)	8.81(-1)	8.70(-1)	8.95(-1)	8.73(-1)
Si^{29}	2.14(-3)	1.77(-3)	9.51(-4)	2.72(-4)	2.82(-3)	1.32(-3)	1.15(-3)	1.16(-3)	8.79(-4)	1.93(-3)
Si^{30}	7.12(-4)	2.30(-4)	6.09(-5)	1.78(-5)	2.02(-2)	7.44(-3)	5.22(-3)	4.05(-3)	3.23(-3)	1.60(-2)
P^{31}	5.26(-4)	3.15(-4)	1.73(-4)	1.15(-4)	1.82(-3)	1.12(-3)	9.90(-4)	8.99(-4)	7.78(-4)	1.48(-3)
S^{32}	4.68(-1)	4.77(-1)	4.25(-1)	3.80(-1)	3.44(-2)	5.39(-2)	6.00(-2)	5.91(-2)	6.47(-2)	4.21(-2)
S^{33}	8.36(-3)	7.38(-3)	4.07(-3)	1.19(-3)	4.34(-4)	3.33(-4)	3.23(-4)	3.18(-4)	2.65(-4)	3.87(-4)
S^{34}	7.81(-2)	3.40(-2)	1.07(-2)	2.37(-3)	4.85(-2)	3.38(-2)	2.70(-2)	1.97(-2)	1.91(-2)	4.85(-2)
Cl^{35}	9.64(-4)	8.64(-4)	6.34(-4)	3.81(-4)	1.73(-4)	1.59(-4)	1.58(-4)	1.41(-4)	1.36(-4)	1.42(-4)
$Cl^{37}(Ar^{37})$	1.23(-4)	3.00(-4)	4.94(-4)	3.56(-4)	9.91(-6)	8.52(-6)	8.89(-6)	7.85(-6)	7.84(-6)	7.94(-6)
Ar^{36}	2.64(-2)	6.28(-2)	1.04(-1)	1.07(-1)	3.43(-4)	7.25(-4)	9.11(-4)	8.86(-4)	1.06(-3)	3.91(-4)
Ar^{38}	3.14(-2)	1.67(-2)	6.56(-3)	4.13(-3)	5.41(-3)	5.53(-3)	4.63(-3)	3.14(-3)	3.43(-3)	6.54(-3)
K^{39}	3.98(-4)	4.36(-4)	3.96(-4)	6.66(-4)	1.98(-5)	2.68(-5)	2.82(-3)	2.32(-5)	2.53(-5)	1.98(-5)
K^{40}	3.86(-8)	3.54(-8)	2.30(-8)	1.86(-8)	3.66(-9)	2.04(-9)	1.87(-9)	1.62(-9)	1.23(-9)	2.28(-9)
$K^{41}(Ca^{41})$	1.45(-5)	5.65(-5)	9.44(-5)	1.21(-4)	1.35(-7)	1.89(-7)	2.18(-7)	2.02(-7)	1.97(-7)	1.25(-7)
Ca^{40}	1.88(-3)	7.66(-3)	1.97(-2)	7.38(-2)	1.83(-5)	5.48(-5)	7.19(-5)	6.50(-5)	8.64(-5)	2.42(-5)
Ca^{42}	8.74(-4)	6.83(-4)	3.12(-4)	1.74(-4)	9.58(-6)	1.28(-5)	1.20(-5)	8.34(-6)	9.05(-6)	1.22(-5)

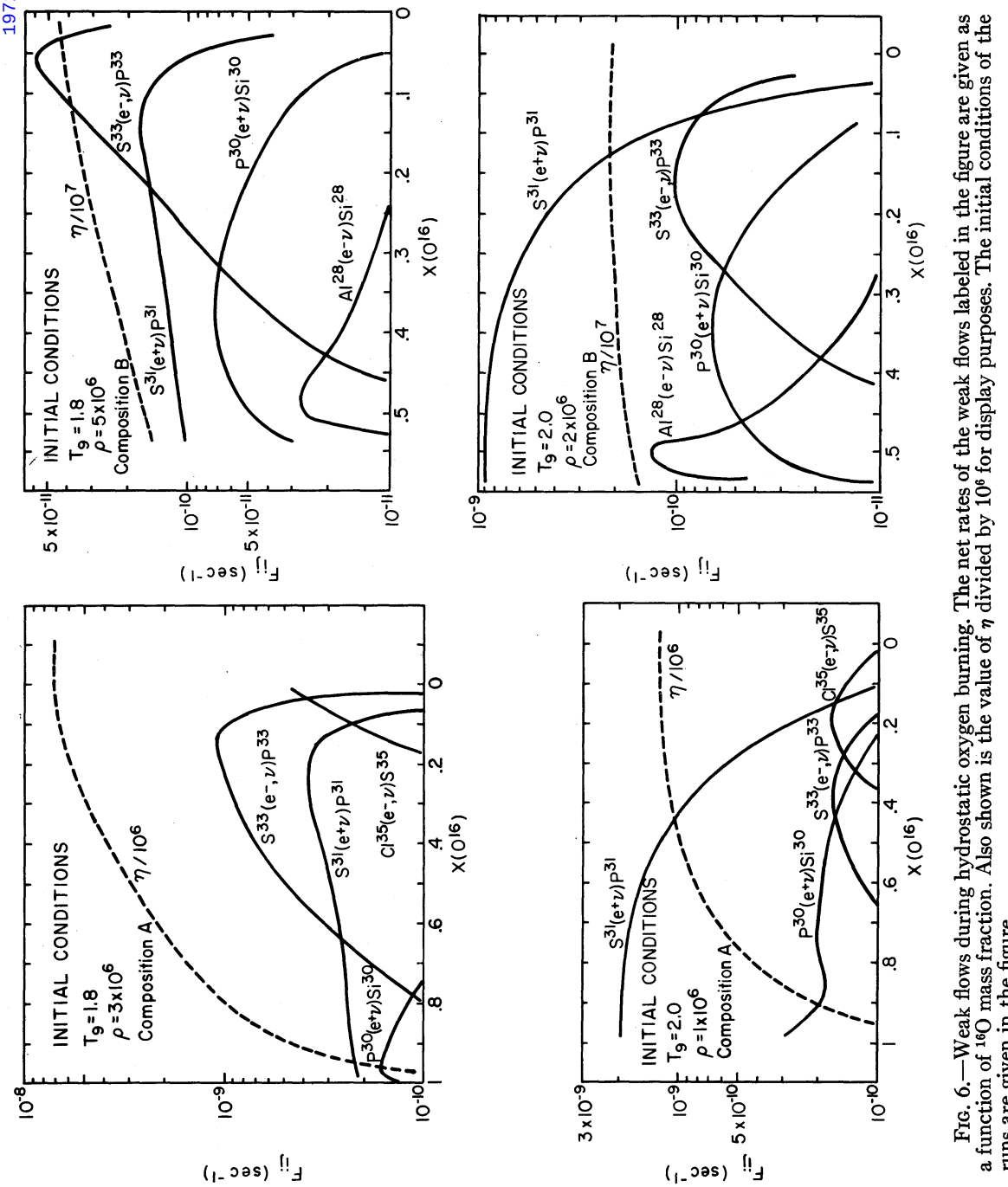

FIG. 6.—Weak flows during hydrostatic oxygen burning. The net rates of the weak flows labeled in the figure are given as a function of ^{16}O mass fraction. Also shown is the value of η divided by 10^6 for display purposes. The initial conditions of the runs are given in the figure.

this reaction is only important for composition B (and other compositions containing sizable amounts of ^{24}Mg), and at temperatures low enough that ^{27}Al$(n, \gamma)^{28}$Al dominates ^{27}Al$(p, \gamma)^{28}$Si. For the cross-sections given in table 2 the rate of ^{28}Al$(e^-\bar{\nu})^{28}$Si is about 5 times too small to effectively retard the increase in η caused by positron emission and electron capture on other species.

The two chief flows that lead to the increased values of η are ^{31}S$(e^+\nu)^{31}$P and ^{33}S$(e^-, \nu)^{33}$P, the latter being important at lower temperatures after a sizable fraction of the oxygen has burned. The ^{31}S is produced directly via the neutron channel of oxygen burning and is destroyed at low temperatures almost solely by positron emission. The other major means of destroying ^{31}S during hydrostatic oxygen burning is ^{31}S$(\gamma, p)^{30}$P. For the conditions under consideration here the lifetime of ^{31}S against positron emission given by the calculations of Hansen (1968) is roughly 4 seconds, independent of temperature and density. In the temperature range between $T_9 = 1.8$ and $T_9 = 2.1$ the photodisintegration rate of ^{31}S is approximately $3.0 \times 10^{-14} T_9^{41}$ s^{-1}; thus

$$\frac{\lambda_{\beta^+}(^{31}\mathrm{S})}{\lambda_{\gamma p}(^{31}\mathrm{S})} \approx 3.6 \left(\frac{T_9}{2}\right)^{-41} .$$

The decay of ^{31}S by positron emission will lead to a change in η over the course of oxygen burning equal to

$$\Delta\eta(^{31}\mathrm{S}) = (2)(B_n)(\tfrac{1}{2}\Delta Y_{16})(f_{\beta^+}) , \qquad (5)$$

where B_n is the neutron branching ratio of oxygen burning, ΔY_{16} is the amount of ^{16}O consumed during the run, and f_{β^+} is the fraction of ^{31}S nuclei destroyed by positron emission. We take the neutron branching ratio here (from the Spinka and Winkler 1972 data) to be 0.048. Assuming all the initial ^{16}O is consumed in hydrostatic oxygen burning then gives an upper bound to $\Delta\eta$ by this process:

$$\Delta\eta_{\max}(^{31}\mathrm{S}) = (2)(0.048)\left[\frac{X_i(^{16}\mathrm{O})}{32}\right]\left[1 + 0.28\left(\frac{T_9}{2}\right)^{41}\right]^{-1}$$

$$= 2.88 \times 10^{-3}\left[1 + 0.28\left(\frac{T_9}{2}\right)^{41}\right]^{-1} X_i(^{16}\mathrm{O}) ,$$

where $X_i(^{16}\mathrm{O})$ is the initial ^{16}O mass fraction. For composition B this would give a theoretical increase of $\Delta\eta = 1.56 \times 10^{-3}$ if $T_9 \lesssim 2.0$. Table 3 shows that for η initially equal to zero (i.e., composition C) and an initial temperature $T_9 = 1.9$ the neutron enrichment is approaching this value quite closely. For compositions with an initial neutron excess which is substantial, the neutron density during the evolution will be high enough that (n, γ) reactions will partially destroy ^{31}S, thereby lowering f_{β^+} resulting in a lower value for $\Delta\eta$ for initial compositions B and D at the same temperature.

It is interesting to note that for $\Delta X(^{16}\mathrm{O}) = 1.0$ the value of $\Delta\eta$ given by equation (5) is very nearly the value needed for η to ensure that subsequent explosive processing yields a distribution comparable to solar-system abundances. Thus, if for some reason a star commenced oxygen burning without any initial neutron excess and a composition of nearly pure oxygen, hydrostatic burning at a temperature between $T_9 = 1.8$ (below which electron capture on ^{33}S becomes dominant) and $T_9 = 2.0$, the result would be an increase in η of very nearly the right amount. Since this temperature range spans the conditions encountered throughout the greater part of hydrostatic oxygen burning by a large range of masses of the oxygen stars discussed in Paper I, it may be that the value of η needed for the correct explosive nucleosynthesis in these zones occurs quite naturally. However, the reaction rates involved, particularly the neutron branching ratio for oxygen burning, should undergo further examination before this conclusion is firm. A similar "funneling" of the values of the neutron excess to approximately the required

value was also found to occur during hydrostatic carbon burning by Arnett and Truran (1969). There an approximate balance between the reaction sequences ^{20}Ne(p, γ)^{21}Na(e^+ ν)^{21}Ne(α, n)^{24}Mg and ^{23}Na(n, γ)^{24}Na($e^-\bar{\nu}$)^{24}Mg led to values of η near 0.002 for a wide range of temperatures.

Although significant, the amount of neutron enrichment given by equation (5) is not prohibitive. For further increase in η, electron capture must occur. Electron capture will occur on ^{33}S if the timescale for electron capture, which is a function of temperature and density in this case, becomes much shorter than the oxygen-burning timescale. How much shorter will depend on the abundance of ^{33}S. A change in η of 0.002 beyond the amount produced by the positron emission of ^{31}S would probably be prohibitive. The change in η in a time Δt due to electron capture by ^{33}S is given by

$$\Delta\eta(^{33}\mathrm{S}) \approx 2 Y_{33} \lambda_\epsilon(^{33}\mathrm{S}) \Delta t ,$$

where Y_{33} is the abundance of ^{33}S and $\lambda_\epsilon(^{33}\mathrm{S})$ is its electron-capture rate. The change unacceptably exceeds $\Delta\eta = 0.002$ if

$$\tau_{16}(^{16}\mathrm{O}) > [30\langle X(^{33}\mathrm{S})\rangle \lambda_\epsilon(^{33}\mathrm{S})]^{-1} , \tag{6}$$

where $\tau_{16}(^{16}\mathrm{O}) = Y_{16}/2R_{16}$ is a typical time for the duration of oxygen burning, R_{16} is the rate of the oxygen-burning reaction, and $\langle X(^{33}\mathrm{S})\rangle$ is the average mass fraction of ^{33}S during the time when electron capture is important. For composition A, the quantity $\langle X(^{33}\mathrm{S})\rangle$ has a value of about 5×10^{-3}; for composition B, 2×10^{-3}. Thus electron capture becomes prohibitive for $\tau_{16}(^{16}\mathrm{O}) > 6\tau_\epsilon(^{33}\mathrm{S})$ and $\tau_{16}(^{16}\mathrm{O}) > 16\tau_\epsilon(^{33}\mathrm{S})$, respectively. Lines of constant $\tau_\epsilon(^{33}\mathrm{S})/\tau_{16}(^{16}\mathrm{O})$ are plotted in figure 7. The line $\tau_\epsilon(^{33}\mathrm{S}) = 0.1\ \tau_{16}(^{16}\mathrm{O})$ represents a boundary such that if a zone were to spend a significant fraction of the burning time on the low-temperature side of this line, the neutron excess of that zone would probably be too high. It is worth noting that the chief depopulation mechanism of ^{33}S is ^{33}S(n, α)^{30}Si. This is on the order of, but somewhat larger than, the electron-capture rate. The rate employed for ^{33}S(n, α)^{30}Si is not an experimentally determined number but is due to a calculation based on nuclear systematics performed by Truran (1971). A significant change in this rate could affect somewhat $\langle X(^{33}\mathrm{S})\rangle$ and hence $\Delta\eta$ for a given set of conditions. Laboratory measurement of this cross-section would be useful for a more accurate determination of $\Delta\eta$ for a given nuclear evolution.

Also shown in figure 7 are lines of "balanced power" for the two different oxygen abundances appropriate to the compositions under consideration. These are points which satisfy equation (4) and comprise the set of initial conditions which may be employed under the assumptions of this model. Therefore, the intersection of these lines with the line $\tau_\epsilon(^{33}\mathrm{S}) = 0.1\tau_{16}(^{16}\mathrm{O})$ gives us an approximate lower bound to the ignition temperature for a zone that is not to undergo prohibitive amounts of electron capture. It is useful to express this in terms of the quantity h where $h = T_9/\rho_6^{1/3}$. From the figure we find that the minimum value of h is about 1.35. This ratio is interesting because it can be related to the mass of the oxygen burning core. From an examination of table 1 of Paper I, we find that the value of h during oxygen burning in a star of mass M can be very well fitted by an equation of the form:

$$h = 0.33(\mu\beta)(M/M_\odot)^{2/3} , \tag{7}$$

where μ is the atomic weight per electron (taken equal to 2) and β is evaluated from the standard model (Chandrasekhar 1957). The constant 0.33 depends, in general, on the neutrino loss rate and the rate of nuclear energy generation (and hence the ^{16}O abundance). Evaluating this equation for $h \geq 1.35$, we find that the oxygen star should have a mass of at least $M \geq 2\ M_\odot$. This conclusion is reinforced by a comparison of the thermodynamic history of the balanced-power run (which ignited oxygen at $T_9 = 1.8$ and led to a prohibitive increase in η) with the thermodynamic history of the 2 $M_\odot$ and 4

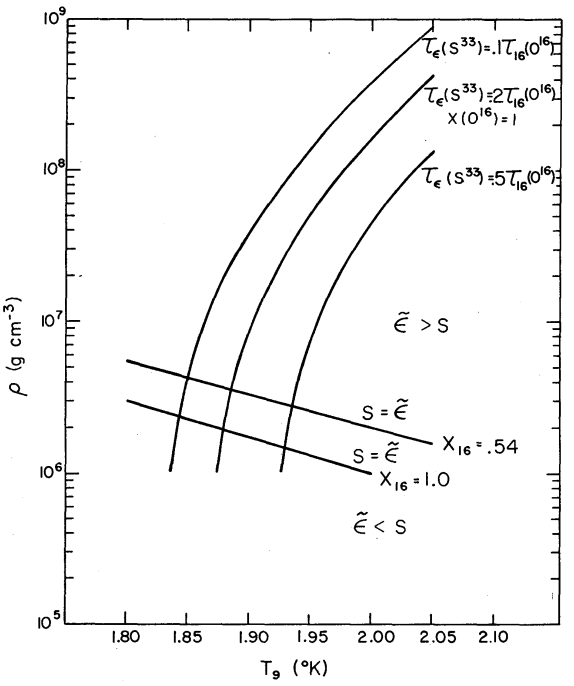

FIG. 7

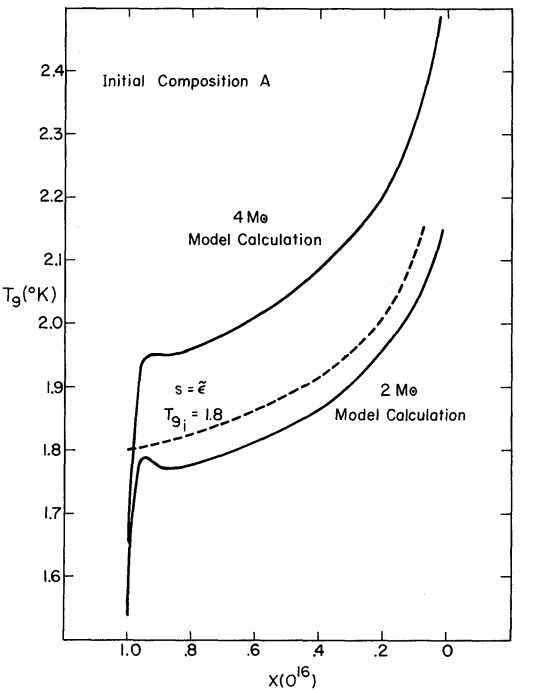

FIG. 8

FIG. 7.—Electron-capture timescales versus oxygen burning timescales. The locus of points in the (ρ, T_9)-plane given by the condition that the timescale for electron capture on ^{33}S be a given fraction of the ^{16}O lifetime against oxygen burning is displayed. The lines shown were drawn assuming that the composition was one of pure oxygen. For other values of $X(^{16}O)$ the fraction in front of $\tau_{16}(^{16}O)$ in the figure should be multiplied by the actual value of $X(^{16}O)$. Also shown are lines of balanced power for the two initial compositions A and B.

FIG. 8.—Thermal history of two oxygen-burning stars. The temperature history of the typical zone of two stellar models that were evolved in Paper I through hydrostatic oxygen burning is shown as a function of the ^{16}O mass fraction. Also shown is the thermal history of the balanced-power run that employed initial condition A and an initial temperature of $T_9 = 1.8$.

$M_\odot$ evolution examined in Paper I. The comparison is shown in figure 8. The temperature of the "balanced-power run" is seen to be an upper bound to that of the 2 $M_\odot$ evolution through oxygen burning. Moreover, the density of the balanced-power run is found to always be a lower bound to the actual density of the 2 $M_\odot$ model (not shown in the figure). If anything, *more* electron capture would occur in the model than in the balanced-power run, which from table 2 is already known to give too large an increase in η. The 4 $M_\odot$ star, on the other hand, evolved in a region that appears allowable. Some neutron enrichment by $^{31}S(e^+\nu)^{31}P$ would be likely, but the effect of electron capture on ^{33}S should be much less pronounced. In short, the nucleosynthesis results of hydrostatic oxygen burning in a 4 $M_\odot$ star of pure ^{16}O would appear to be acceptable for ejection while those of a 2 $M_\odot$ star would not. Any estimate of what mass is ejected would require an investigation of the terminal evolution of the star and would also include previous burning stages (helium, carbon, and neon burning, for example).

V. IMPLICATIONS FOR e-ν COUPLING

The results that we have calculated here have all explicitly assumed the existence of an electron-neutrino coupling that gives rise to a loss of energy whose rate is given approximately by the fitted formulae of Beaudet *et al.* (1967). If the weak-interaction theory is correct, the error introduced by assuming their form for the total neutrino

losses is probably less than the error involved in the balanced-power assumption itself. Moreover, an error of a factor of 3 in equation (1) (see Paper I) would introduce an error of only about 4 percent in the determination of the burning temperature. Thus, our minimum value for the "allowable" ignition temperatures for an oxygen star may be in error by about $\pm 0.07 \times 10^9$ ° K with respect to the calculations in Paper I. An error of this size would not change the qualitative nature of our results. There would still exist some minimum oxygen star mass, in the vicinity of 2 $M_\odot$, that can yield a final value of $\eta < 0.004$ so long as a loss term on the order of what we have assumed for neutrino emission exists. The prime uncertainty in the actual size of the minimum core mass relates to the initial ^{16}O abundance.

If the direct e-ν coupling term does not exist, however, we should obtain very different results. The rate of energy loss from the star would be much lower than what we have assumed, because it would be limited by the rate at which photons could emit from the surface of the oxygen star. The much lower rate of loss would imply a much lower rate of energy generation, and hence a much lower burning temperature. An estimate of the conditions that would prevail in such a star has been obtained from analysis of models evolved without neutrino losses. Their average rate of energy generation is found to be well represented by

$$\langle \epsilon \rangle \equiv L/M$$
$$\simeq 9.0 \times 10^4 (M/M_\odot)^2 \text{ ergs g}^{-1} \text{ s}^{-1}$$

in the range of masses under discussion. Moreover, the ratio of the average rate to the central rate of energy generation can be obtained by using the method of Fowler and Hoyle (1964; see Paper I, eqs. [5] and [6]), with $m \sim 35$ and $u = 2$. Then we have

$$\langle \epsilon \rangle / \epsilon_0 \approx 0.0184 ,$$

and hence

$$\epsilon_0 = 5.1 \times 10^6 (M/M_\odot)^2 \text{ ergs g}^{-1} \text{ s}^{-1} .$$

If we represent ϵ_0 by the energy-generation rate due to $^{16}O + {}^{16}O \rightarrow {}^{32}S$, that is, $\tilde{\epsilon}$, and employ equation (7) to relate ρ and T_9 to the mass of the oxygen star, then we can predict the evolutionary history of an oxygen star of given mass without neutrino losses. The constant 0.33 in equation (7) is obtained if the neutrino rates of Beaudet *et al.* (1967) are used; if energy loss were by radiative transfer, the constant would be 0.492 in the temperature range around $T_9 \approx 1.6$. In the latter case the constant is independent of initial composition. The results are shown in table 4.

Comparison of these numbers with those tabulated in table 1 of Paper I shows that a star which burns oxygen with no neutrino losses will have temperatures some 0.4 billion degrees cooler and densities a factor of 5 lower than the same star with neutrino losses included. Comparison with the various balanced-power runs implies that the stars listed in table 4 can all be expected to have large increases in η during their evolution. Even a 16 $M_\odot$ oxygen star would yield values of $\Delta\eta$ so large that explosive processing would probably result in elemental abundances that differed greatly from the solar-system distribution. The actual mass of a star having a 16 $M_\odot$ oxygen core would be much greater than 16 $M_\odot$. Thus we see that it would take a massive star indeed to give $\Delta\eta < 0.004$ during the hydrostatic burning of an oxygen core. Conditions are improved slightly if the composition of the core is not pure oxygen but is rather the result of hydrostatic carbon burning (e.g., composition B). Then the temperature in the "no neutrino" case is about 0.05 billion degrees hotter and the density a little lower than the pure ^{16}O case. But inspection of table 4 shows that even if the temperature were 0.05 larger in T_9, the electron capture would still be prohibitive in all stars considered.

The theoretical models considered here are quite simple, and their relation to real stars may not be obvious. Nevertheless, they do strongly suggest the existence of an

TABLE 4

TEMPERATURE AND DENSITY HISTORIES OF HYDROSTATIC OXYGEN BURNING WITH NO NEUTRINO LOSSES

	$2\,M_\odot$		$4\,M_\odot$		$8\,M_\odot$		$16\,M_\odot$	
$X(^{16}O)$	ρ_6	T_9	ρ_6	T_9	ρ_6	T_9	ρ_6	T_9
1.0.....	1.23	1.47	0.589	1.56	0.345	1.64	0.226	1.73
0.9.....	1.25	1.48	0.598	1.57	0.351	1.65	0.230	1.74
0.8.....	1.27	1.49	0.610	1.58	0.358	1.66	0.234	1.75
0.7.....	1.30	1.50	0.622	1.59	0.365	1.68	0.239	1.76
0.6.....	1.33	1.51	0.636	1.60	0.374	1.69	0.245	1.78
0.5.....	1.36	1.52	0.655	1.62	0.385	1.71	0.252	1.80
0.4.....	1.41	1.54	0.678	1.63	0.399	1.73	0.262	1.82
0.3.....	1.48	1.56	0.710	1.66	0.418	1.75	0.274	1.85
0.2.....	1.57	1.60	0.755	1.69	0.445	1.79	0.293	1.89
0.1.....	2.52	1.87	1.227	1.99	0.731	2.11	0.527	2.29

energy-loss mechanism which is much more effective than photon diffusion. If much matter processed by hydrostatic oxygen burning in stellar centers is ever ejected into the interstellar medium, then it must have been processed under conditions very like those obtained by assuming that a direct e-ν coupling exists. The "η" argument given above is supported by the structure argument given in Paper I. While astrophysical arguments are no substitute for weak-interaction experiments, it is interesting that the assumption that a direct e-ν interaction exists removes some theoretical difficulties.

VI. SUMMARY

We have examined in detail the nucleosynthesis that would be expected to occur during hydrostatic oxygen burning for a range of ignition temperatures, $1.8 \leq T_9 \leq 2.2$, under the assumption of an approximate balance between nuclear energy generation and neutrino losses. We find that such zones yield a composition at the onset of silicon burning chiefly comprised of elements in the $28 \leq A \leq 40$ mass range and characterized by a range of neutron mass excesses which increase as the ignition temperature for the burning (or the core mass) decreases. The actual resultant composition, though tabulated, is not immediately applicable to natural abundances, as we would expect it to be greatly modified by any subsequent processing that results in ejection into the interstellar medium. A quantity that is of immediate interest, however, is the neutron mass excess η. It is very doubtful that the value of η at the end of hydrostatic oxygen burning will *decrease* in any future burning stage—either hydrostatic or explosive. Thus is the zones under consideration are to undergo explosive processing and be ejected, then the value of η established by oxygen burning should be a lower limit to the η of the explosive ejecta. From past calculations we know that there exist fairly stringent limits on the values η which can characterize a large fraction of the material ejected from supernovae during the past history of the Galaxy. In particular, the zones which we have been discussing, which would be a probable site of explosive silicon burning or of the e-process, should not have a value of η too much greater than 0.002 in order that explosive processing produce an iron-peak abundance distribution similar to the observed solar abundances. We find that this restriction on η implies a minimum ignition temperature for hydrostatic oxygen burning of about 1.8×10^9 ° K that is fairly independent of the initial composition assumed. Imposing this restriction on the models of Paper I leads us to believe that this minimum ignition temperature corresponds to a minimum mass of about 2 $M_\odot$ for a pure ^{16}O star. Stars which ignite ^{16}O in zones at lower

temperatures must either retain such zones in some form of bound remnant or comprise a very small fraction of the ensemble of all past supernova explosions. We find that models which assume the existence of a direct e-ν coupling term in the weak interaction give results upon explosion (if it occurs) that are more consistent with our current ideas regarding stellar nucleosynthesis than models that do not.

As a by-product of this investigation we have determined the accuracy of the simple approximation to the energy-generation rate used in Paper I. We find $\tilde{\epsilon}$ to be a representation of the actual energy-generation rate good to within about 20 percent up until the time of ^{16}O depletion [$X(^{16}O) \lesssim$ a few percent]. We have also identified the nuclear reactions that are of importance to the nucleosynthesis that occurs during hydrostatic oxygen burning. They are listed in table 1. Of special interest are the reactions which govern the change in neutron excess during oxygen burning. These are the reaction $^{16}O + {}^{16}O$ (especially the neutron branching ratio) and all the reactions indicated by an asterisk.

The authors would like to thank Professors William A. Fowler, Hubert Winkler, and Jim Truran and Dr. Harold Spinka for allowing us to use the results of their research prior to publication. We also wish to thank Professor Fred Hoyle and the Institute of Theoretical Astronomy, Cambridge, England, for their hospitality and a generous grant of computer time while this paper was in preparation. This work has been supported in part by the National Science Foundation grants GP-18335 and GP-23459.

REFERENCES

Arnett, W. D. 1969*a*, *Ap. J.*, **157**, 1369.
———. 1969*b*, in *Supernovae and Supernova Remnants*, ed. P. Brancazio and A. G. W. Cameron (New York: Gordon & Breach).
———. 1971, *Ap. J.*, **166**, 153.
———. 1972, submitted to *Ap. J.* (Paper I).
Arnett, W. D., and Clayton, D. D. 1970, *Nature*, **227**, 780.
Arnett, W. D., and Truran, J. W. 1969, *Ap. J.*, **157**, 339.
Beaudet, G., Petrosian V., and Salpeter, E. E. 1967, *Ap. J.*, **150**, 979.
Chandrasekhar, S. 1957, *An Introduction to Stellar Structure* (New York: Dover Publications), p. 229.
Fowler, W. A., Caughlan, G. R., and Zimmerman, B. A. 1971, private communication. See also *Ann. Rev. Astr. and Ap.*, **5**, 525 (1967).
Fowler, W. A., and Hoyle, F. 1964, *Ap. J. Suppl.*, **9**, No. 91, 201.
Hansen, C. J. 1968, *Ap. and Space Sci.*, **1**, 499. (Also Ph.D. dissertation, Yale University, 1967.)
Patterson, J. R., Nagorcka, B. N., Symons, and Zuk, W. M. 1971, *Nucl. Phys.*, **A165**, 545.
Patterson, J. R., Winkler, H., and Zaidins, C. S. 1969, *Ap. J.*, **157**, 367.
Spinka, H., and Winkler, H. 1972, to be published.
Truran, J. W. 1971, private communication. (See also Truran, J. W. 1968, *Ap. and Space Sci.*, **2**, 384 and 391.)
Truran, J. W., and Arnett, W. D. 1970, *Ap. J.*, **160**, 181.
———. 1971, *Ap. and Space Sci.*, **11**, 430.
Woosley, S. E., Arnett, W. D., and Clayton, D. D. 1971, *Phys. Rev. Letters*, **27**, 213.
———. 1972, to be published.